Identification of indirect new physics effects at e^+e^- colliders: The large extra dimensions case

A. A. Pankov*

Pavel Sukhoi Technical University, Gomel 246746, Belarus

N. Paver†

University of Trieste and INFN-Sezione di Trieste, 34100 Trieste, Italy

We discuss indirect manifestations of graviton exchange, predicted by large extra dimensions, in fermion-pair production at a high-energy e^+e^- collider. By means of specifically defined asymmetries among integrated angular distributions, the graviton exchange signal can be cleanly distinguished from the effects of either vector-vector contact interactions or heavy scalar exchanges. The role of initial electron and positron beams polarization is also discussed. The method is applied to a quantitative assessment of the sensitivity to the mass cutoff parameter M_H of the KK graviton tower in the ADD scenario, and of the potential identification reach of this mechanism obtainable at the currently planned International Linear Collider.

PACS numbers: 12.60.Cn, 04.50.+h

I. INTRODUCTION

Although the standard model (SM) of particle physics has been experimentally verified with impressive confirmations, there is both a theoretical belief and mounting phenomenological evidence that this model cannot be considered as the ultimate theory of fundamental interactions. Accordingly, there exists a variety of proposed new physics (NP) scenarios beyond the SM, characterized by different kinds of nonstandard dynamics involving new building blocks and forces mediated by exchanges of new heavy states, generally with mass scales much greater than M_W or M_Z. Searches for such nonstandard scenarios are considered as priorities for experiments at very high energy accelerators.

Clearly, the direct production of the new heavy objects at the Large Hadron Collider (LHC) and at the e^+e^- International Linear Collider (ILC), and the measurement of their couplings to ordinary matter, would allow the unambiguous confirmation of a given NP model. One hopes this to be the case of the supersymmetric (SUSY) extensions to the SM. In many interesting cases, however, the threshold for direct production of the new heavy particles may be much higher than the machine energy. In this situation, the relevant novel interaction can manifest itself only indirectly, via deviations of measured observables from the SM predictions, produced by virtual heavy quantum exchange.

A convenient theoretical representation of this kind of scenario is based on appropriate *effective* local interactions among the familiar SM particles that lead to ''low'' energy expansions of the transition amplitudes in inverse powers of the above mentioned very large mass scales. Such

interaction Hamiltonians are described by specific operators of increasing dimension and, generally, only the lowest-dimension significant operator is retained, assuming the contributions of the higher-dimensional ones to be strongly suppressed by the higher inverse powers of the large mass scale hence negligible. Furthermore, additional criteria and symmetries are imposed in order to fix the phenomenologically viable forms of such nonstandard effective interactions and to limit the number of the new coupling constants and mass scales to be experimentally determined (or constrained).

Since different nonstandard interactions can in principle induce similar deviations of the cross sections from the SM predictions, it is important to define observables designed to identify, among the possible nonstandard interactions, the actual source of a deviation, were it observed within the experimental accuracy.

Great attention has been given, in the context of the hierarchy problem between the Planck and the electroweak mass scales, to scenarios involving compactified extra dimensions. We will here focus on the so-called ADD model where the extra spatial dimensions, in which gravity only can propagate, are of the ''large'' millimeter size [1–3]. Specifically, we will discuss the possibility of uniquely distinguishing, in e^+e^- annihilation into fermion pairs at the Linear Collider, the effects of graviton exchange predicted by this scenario from the, in principle competing, new physics scenarios represented by four-fermion contact effective interactions. While originating in the context of compositeness of quarks and leptons [4–6], the latter can more generally represent a variety of new interactions, generated by exchanges of very heavy new objects such as, e.g., heavy Z', leptoquarks, heavy scalars, with masses much larger than the Mandelstam variables of the considered process.

Since, according to the above considerations, the deviations are suppressed by powers of the ratio between the

*Electronic address: pankov@ictp.it
Abdus Salam ICTP, Strada Costiera 11, 34100 Trieste, Italy
†Electronic address: nello.paver@ts.infn.it

process Mandelstam variables and the square of the large mass scale characteristic of the considered novel interaction, the search for *indirect* manifestations of such new physics will be favored by high energies (and luminosities) that may increase the signal and therefore allow higher sensitivities.

In Ref. [7], a particular combination of integrated cross sections, the so-called "center-edge asymmetry" A_{CE}, was shown to provide a simple tool to exploit the spin-2 character of graviton exchange in high-energy e^+e^- annihilation, and to disentangle this effect from vector-vector contact interactions.[1] This method should usefully complement the ones based on Monte Carlo best fits [9], or on integrated differential cross sections weighted by Legendre polynomials [10].

Here, we shall propose an analysis based on an extension of the above mentioned asymmetry, the "center-edge-forward-backward asymmetry" $A_{CE,FB}$, that should allow the distinction of spin-2 graviton exchange from contact four-fermion interactions, and we will assess the corresponding identification reach obtainable at the planned International Linear Collider. On the other hand, it will be found that the new asymmetry can be used also to determine the discovery reach on the contact interactions free from contamination of graviton exchange, and therefore to extract useful information also on that sector of new physics.

Specifically, in Sec. II the differential cross section and the deviations from the SM induced by the above mentioned NP scenarios are discussed. In Secs. III and IV the basic observable asymmetries are defined, both for unpolarized and for polarized electron and positron beams. The identification reaches on graviton exchange and on four-fermion contact interactions are numerically derived for "standard" linear collider parameters in Sec. V. Finally, a few conclusive remarks are given in Sec. VI.

II. DIFFERENTIAL CROSS SECTIONS

We consider the process (with $f \neq e, t$)

$$e^+ + e^- \rightarrow f + \bar{f} \qquad (2.1)$$

with unpolarized e^+e^- beams. Neglecting all fermion masses with respect to the c.m. energy $\sqrt{s}$, the differential cross section can be written as [11]:

$$\frac{d\sigma}{dz} = \frac{1}{4}\left(\frac{d\sigma_{LL}}{dz} + \frac{d\sigma_{RR}}{dz} + \frac{d\sigma_{LR}}{dz} + \frac{d\sigma_{RL}}{dz}\right). \qquad (2.2)$$

Here, $z \equiv \cos\theta$ with θ the angle between the incoming electron and the outgoing fermion in the c.m. frame, and $d\sigma_{\alpha\beta}/d\cos\theta$ ($\alpha, \beta = L, R$) are the helicity cross sections

---

[1]An application of this method to lepton-pair production at hadron colliders was discussed in Ref. [8].

$$\frac{d\sigma_{\alpha\beta}}{dz} = N_C\frac{3}{8}\sigma_{pt}|\mathcal{M}_{\alpha\beta}|^2(1 \pm z)^2. \qquad (2.3)$$

Conventions are such that the subscripts α and β in the reduced helicity amplitudes $\mathcal{M}_{\alpha\beta}$ indicate the helicities of the initial and final fermions, respectively. In Eq. (2.3), the "+" sign applies to the combinations LL and RR, while the "−" sign applies to the LR and RL cases. Also, $\sigma_{pt} = 4\pi\alpha_{e.m.}^2/3s$, and the color factor $N_C \simeq 3(1 + \alpha_s/\pi)$ is needed only in the case of quark-antiquark final states.

In the SM the helicity amplitudes, representing the familiar s-channel photon and Z exchanges, are given by

$$\mathcal{M}_{\alpha\beta}^{SM} = Q_eQ_f + g_\alpha^e g_\beta^f \chi_Z, \qquad (2.4)$$

where $\chi_Z = s/(s - M_Z^2 + iM_Z\Gamma_Z) \simeq s/(s - M_Z^2)$ for $\sqrt{s} \gg M_Z$; $g_L^f = (I_{3L}^f - Q_f s_W^2)/s_W c_W$ and $g_R^f = -Q_f s_W/c_W$ are the SM left- and right-handed fermion couplings to the Z, with $s_W^2 = 1 - c_W^2 \equiv \sin^2\theta_W$; Q_e and Q_f are the initial and final fermion electric charges. The SM differential cross section can be decomposed into z-even and z-odd parts:

$$\frac{d\sigma^{SM}}{dz} = \frac{3}{8}\sigma^{SM}(1 + z^2) + \sigma_{FB}^{SM}z, \qquad (2.5)$$

where

$$\sigma = \int_{-1}^{1}\frac{d\sigma}{dz}dz \quad \text{and}$$
$$\sigma_{FB} \equiv \sigma A_{FB} = \left(\int_0^1 - \int_{-1}^0\right)\frac{d\sigma}{dz}dz \qquad (2.6)$$

denote the total and the forward-backward cross sections, respectively. In particular, in terms of the amplitudes $\mathcal{M}_{\alpha\beta}^{SM}$:

$$A_{FB}^{SM} = \frac{3}{4}\frac{(\mathcal{M}_{LL}^{SM})^2 + (\mathcal{M}_{RR}^{SM})^2 - (\mathcal{M}_{LR}^{SM})^2 - (\mathcal{M}_{RL}^{SM})^2}{(\mathcal{M}_{LL}^{SM})^2 + (\mathcal{M}_{RR}^{SM})^2 + (\mathcal{M}_{LR}^{SM})^2 + (\mathcal{M}_{RL}^{SM})^2}. \qquad (2.7)$$

Rather generally, in the presence of nonstandard interactions coming from the new, TeV-scale physics, the reduced helicity amplitudes can be expanded into the SM part plus a deviation depending on the considered NP model:

$$\mathcal{M}_{\alpha\beta} = \mathcal{M}_{\alpha\beta}^{SM} + \Delta_{\alpha\beta}, \qquad (2.8)$$

where the quantities $\Delta_{\alpha\beta} \equiv \Delta_{\alpha\beta}(NP)$ represent the contribution of the new interaction. The typical examples relevant to our discussion are as follows.

A. The large extra dimension scenario

We consider the large extra dimension scenario with exchange of Kaluza-Klein (KK) towers of gravitons [1–3]. In this new physics scenario, gravity propagates in two or more extra spatial dimensions, compactified to a size R_c of the millimeter order.[2] In four dimensions, this translates to a tower of KK graviton states with evenly spaced (and almost continuous) mass spectrum $m_{\vec{n}} = \sqrt{\vec{n}^2/R_c^2}$, where $\vec{n}$ labels the KK states. The Feynman rules for KK vertices were given in Refs. [12,13]. The exchange of such an object is described by a dimension-8 effective Lagrangian, and we here choose the form [14]:

$$\mathcal{L}^{\mathrm{ADD}} = i\frac{4\lambda}{M_H^4}T^{\mu\nu}T_{\mu\nu}. \qquad (2.9)$$

In Eq. (2.9), $T_{\mu\nu}$ is the stress-energy tensor of the SM particles, M_H is a cutoff on the summation over the KK spectrum, expected to be in the TeV range, and $\lambda = \pm 1$.[3] To avoid confusion with the notations, the input SM Higgs mass will in the sequel be denoted by m_H. The corresponding deviations of the helicity amplitudes for the e^+e^- annihilation process (2.1) under consideration, defined in Eq. (2.8), can be written as

$$\Delta_{\mathrm{LL}}(\mathrm{ADD}) = \Delta_{\mathrm{RR}}(\mathrm{ADD}) = f_G(1 - 2z), \\ \Delta_{\mathrm{LR}}(\mathrm{ADD}) = \Delta_{\mathrm{RL}}(\mathrm{ADD}) = -f_G(1 + 2z), \qquad (2.10)$$

where $f_G = \lambda s^2/(4\pi\alpha_{\mathrm{e.m.}}M_H^4)$ parametrizes the strength associated with massive, spin-2, graviton exchange.

Concerning the current experimental limits on M_H, from the nonobservation of deviations from graviton exchange at LEP2 the strongest limits are $M_H > 1.20$ TeV for $\lambda = +1$ and $M_H > 1.09$ TeV for $\lambda = -1$ [16]. In hadron-hadron collisions, virtual graviton exchange modifies the dilepton and diphoton production cross sections. The combined limit obtained by the CDF and D0 Collaborations at the Tevatron Run II $p\bar{p}$ collider is: $M_H > 1.28$ TeV [17,18]. Experiments at the LHC are expected to be able to explore extra dimensions up to multi-TeV scales [19,20].

B. Contact interactions

We consider the four-fermion contact interactions, such as the vector-vector ones envisaged in composite models [4–6]. These are described by the leading dimension-6 operators,

$$\mathcal{L}_{\mathrm{CI}} = 4\pi\sum_{\alpha,\beta}\frac{\eta_{\alpha\beta}}{\Lambda_{\alpha\beta}^2}(\bar{e}_\alpha\gamma_\mu e_\alpha)(\bar{f}_\beta\gamma^\mu f_\beta), \qquad (2.11)$$

where Λ's are compositeness mass scales and $\eta_{\alpha\beta} =$

$\pm 1, 0$. Accordingly,

$$\Delta_{\alpha\beta}(\mathrm{CI}) = \pm\frac{s}{\alpha_{\mathrm{e.m.}}}\frac{1}{\Lambda_{\alpha\beta}^2}. \qquad (2.12)$$

Current limits on Λ's for the specific helicity combinations are model-dependent and significantly vary according the process studied and the kind of analysis performed there. In general, results from global analyses are given, and the lower limits are of the order of 10 TeV. A detailed presentation of the situation can be found in the listings of Ref. [21].

As previously mentioned, other new physics scenarios can in principle mimic the virtual effects of massive graviton exchange as well as those of contact interactions, *via* the produced deviations of cross sections from the SM predictions. As a representative example, we choose here to discuss the case of a heavy scalar exchange in the t-channel of process (2.1) with $f = \mu$ and τ, such as the sneutrino $\tilde{\nu}$ relevant to R-parity breaking SUSY interactions [22,23]. In this case, the additional contributions to helicity amplitudes in Eq. (2.8) can be written in the form

$$\Delta_{\mathrm{LL}}(\tilde{\nu}) = \Delta_{\mathrm{RR}}(\tilde{\nu}) = 0, \\ \Delta_{\mathrm{RL}}(\tilde{\nu}) = \Delta_{\mathrm{LR}}(\tilde{\nu}) = \frac{1}{2}C_{\tilde{\nu}}\frac{s}{t - m^2}. \qquad (2.13)$$

Here, m is the sneutrino mass, $C_{\tilde{\nu}} = \lambda^2/4\pi\alpha_{\mathrm{e.m.}}$ with λ a Yukawa coupling, and $t = -s(1 - z)/2$.[4] According to Eq. (2.13), the LL and RR amplitudes are completely free from $\tilde{\nu}$-exchange, whereas the RL and LR ones *are* affected. Indeed, in the heavy sneutrino limit $s, -t \ll m^2$ assumed here, the deviations in leading order behave like the contact four-fermion interaction ones in Eq. (2.12) and, in particular, are z-independent. Only at the next order the propagator effects induced by t/m^2 can introduce an (expectably suppressed) angular dependence of the deviations analogous to Eq. (2.10).

Restrictions from low-energy experiments can be summarized by the inequality $\lambda \lesssim 0.1 \times (m/200 \text{ GeV})$ [22]. Considering the equivalence $m/\lambda \sim \Lambda/\sqrt{8\pi}$ obtained by comparing Eqs. (2.13) and (2.12) in the contact interaction limit, current limits on Λ's in the lepton sector of the order of 10 TeV, as obtained from LEP2, can be translated to $m > 2\lambda$ TeV.

III. CENTER–EDGE ASYMMETRIES

A. The center-edge asymmetry A_{CE}

We define the generalized center-edge asymmetry A_{CE} as [7,24]

$$A_{\mathrm{CE}} = \frac{\sigma_{\mathrm{CE}}}{\sigma}, \qquad (3.1)$$

---

[2]Actually, two extra dimensions for the ADD scenario is close to bounds set by gravitational and cosmological experiments.

[3]In principle, the notion of minimal length scale, of order TeV^{-1}, as a smooth cutoff on the summation over the KK states, can be incorporated in the ADD scenario [15].

---

[4]In principle, a situation where there are sneutrino exchanges in both the s- and t-channels may occur [22,23].

where σ_{CE} is the difference between the "central" and "edge" parts of the cross section, with $0 < z^* < 1$

$$\sigma_{\text{CE}}(z^*) = \left[\int_{-z^*}^{z^*} - \left(\int_{-1}^{-z^*} + \int_{z^*}^{1} \right) \right] \frac{d\sigma}{dz} dz. \qquad (3.2)$$

The integration range relevant to Eq. (3.2) is depicted in Fig. 1.

Clearly, from the definition Eq. (3.2), $\sigma_{\text{CE}} = \mp \sigma$ at $z^* = 0$ and 1, respectively. Furthermore, z-odd terms in the differential cross section cannot contribute to A_{CE}.

Using Eq. (2.5), one immediately obtains in the SM:

$$A_{\text{CE}}^{\text{SM}}(z^*) = \frac{1}{2} z^*(z^{*2} + 3) - 1, \qquad (3.3)$$

independent of the c.m. energy $\sqrt{s}$, of the flavor of final fermions and of the longitudinal beams polarization (which will be considered later).

From the decomposition (2.8), one can write $A_{\text{CE}}(z^*)$ as follows:

$$A_{\text{CE}} = \frac{\sigma_{\text{CE}}^{\text{SM}} + \sigma_{\text{CE}}^{\text{INT}} + \sigma_{\text{CE}}^{\text{NP}}}{\sigma^{\text{SM}} + \sigma^{\text{INT}} + \sigma^{\text{NP}}}, \qquad (3.4)$$

where "SM," "INT," and "NP" refer to "standard model," "interference," and (pure) "new physics" contributions.

One can quite easily verify, from Eq. (2.12), that in the case where current-current contact interactions are present in addition to the SM ones, the z-dependence of the resulting differential cross section has exactly the same structure as that of Eq. (2.5), up to the superscripts replacement SM $\rightarrow$ CI. Consequently, A_{CE} in this case is identical to the SM one, i.e., to Eq. (3.3),

$$A_{\text{CE}}^{\text{CI}}(z^*) = \frac{1}{2} z^*(z^{*2} + 3) - 1. \qquad (3.5)$$

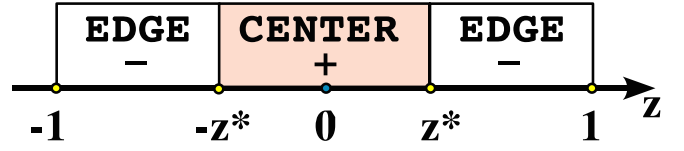Introducing, in general, the deviation of A_{CE} from the SM prediction,

FIG. 1 (color online). The kinematical range of $z \equiv \cos\theta$ and the three bins, one center and two edge ones, used in the definition of center-edge asymmetry A_{CE}.

$$\Delta A_{\text{CE}} = A_{\text{CE}} - A_{\text{CE}}^{\text{SM}}, \qquad (3.6)$$

in the case of "conventional" contact interactions

$$\Delta A_{\text{CE}}^{\text{CI}} = 0, \qquad (3.7)$$

for any value of z^*. Correspondingly, such interactions are "filtered out" by the asymmetry (3.1), in the sense that they produce *no* deviation from the SM prediction. One can easily see that this is the reflection of the postulated vector-vector character of Eq. (2.11) and the consequent z-independence of the right-hand side of Eq. (2.12).

Furthermore, Eqs. (3.3) and (3.5) show that $A_{\text{CE}}^{\text{SM}} = A_{\text{CE}}^{\text{CI}}$ vanish [7,25], at

$$z_0^* = (\sqrt{2} + 1)^{1/3} - (\sqrt{2} - 1)^{1/3} = 0.596, \qquad (3.8)$$

corresponding to $\theta = 53.4°$.

Spin-2 KK graviton exchange provides characteristic z-dependent deviations of helicity amplitudes, see Eq. (2.10), and *nonzero* values of ΔA_{CE}. In addition, for this kind of new interaction, $\sigma^{\text{INT}} = 0$ in the denominator of Eq. (3.4) and the pure NP contributions proportional to f_G^2 should be strongly suppressed by the high power $(\sqrt{s}/M_H)^8$, where $(\sqrt{s}/M_H)^4$ is assumed to be much smaller than unity. Therefore, a linear (in f_G) approximation to Eq. (3.4) should numerically be a good approximation and, accordingly, one readily derives the expression

$$\Delta A_{\text{CE}}^{\text{ADD}}(z^*) = \frac{3}{4} f_G \frac{\mathcal{M}_{\text{LL}}^{\text{SM}} + \mathcal{M}_{\text{RR}}^{\text{SM}} - \mathcal{M}_{\text{LR}}^{\text{SM}} - \mathcal{M}_{\text{RL}}^{\text{SM}}}{[(\mathcal{M}_{\text{LL}}^{\text{SM}})^2 + (\mathcal{M}_{\text{RR}}^{\text{SM}})^2 + (\mathcal{M}_{\text{LR}}^{\text{SM}})^2 + (\mathcal{M}_{\text{RL}}^{\text{SM}})^2]} 4z^*(1 - z^{*2}). \qquad (3.9)$$

In Fig. 2, the z^* dependence of A_{CE} is shown either for the SM or the CI models and for the ADD scenario (for particular values of M_H). One can conclude that the non-vanishing $\Delta A_{\text{CE}} \neq 0$ at arbitrary values of z^* (except $z^* = 0, 1$), or even $A_{\text{CE}} \neq 0$ itself for z^* in a range around z_0^*, unambiguously signal the presence of new physics *different* from contact four-fermion interactions.

These considerations have been used in Ref. [7] to assess the reach on the determination of the ADD graviton exchange process with the result that, depending on the linear collider parameters (such as c.m. energy, luminosity, beams polarizations) and on the final states considered, the potentially reachable sensitivities to the values of the scale parameter M_H are in the range of 4–5 TeV at the

planned ILC with $\sqrt{s} = 500$ GeV [26], up to 10–15 TeV at a Compact Linear Collider (CLIC) with $\sqrt{s} = 3 - 5$ TeV [27].

B. The center−edge−forward−backward asymmetry $A_{\text{CE,FB}}$

Still with unpolarized beams, we define this asymmetry as follows:

$$A_{\text{CE,FB}} = \frac{\sigma_{\text{CE,FB}}}{\sigma}, \qquad (3.10)$$
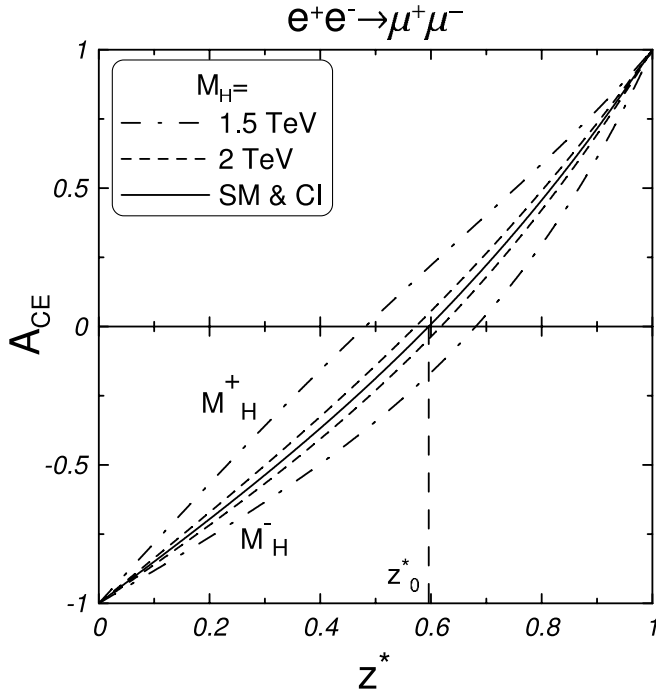
where, with $0 < z^* < 1$,

$$e^+e^- \rightarrow \mu^+\mu^-$$

FIG. 2. Center-edge asymmetry A_{CE} for $e^+ e^- \rightarrow \mu^+ \mu^-$ vs z^* in the SM and with CI (solid line) and in the ADD scenario with $M_{\bar{H}}^+ = 1.5$ TeV (dot-dashed lines) and $M_{\bar{H}}^+ = 2$ TeV (dashed lines). The $\pm$ superscripts correspond to constructive and destructive interference of the SM amplitudes with the graviton exchange.

$$\sigma_{CE,FB} = \left[\left(\int_0^{z^*} - \int_{-z^*}^0 \right) - \left(\int_{z^*}^1 - \int_{-1}^{-z^*} \right) \right] \frac{d\sigma}{dz} dz$$
$$\equiv (\sigma_{C,FB} - \sigma_{E,FB}). \qquad (3.11)$$

For illustrative purposes, the integration range relevant to Eq. (3.11) is shown in Fig. 3. Clearly, z-even terms in the differential cross section do not contribute to Eq. (3.10). Also, by definition, $A_{CE,FB}(z^* = 1) = A_{FB}$ and $A_{CE,FB}(z^* = 0) = -A_{FB}$.

In the SM, using Eq. (2.5) one immediately derives

$$A_{CE,FB}^{SM}(z^*) = A_{FB}^{SM}(2z^{*2} - 1), \qquad (3.12)$$

where the expression of A_{FB}^{SM} in terms of the helicity amplitudes is given in Eq. (2.7).

One can immediately see from Eq. (2.12) that in the case of the conventional current-current contact interactions,
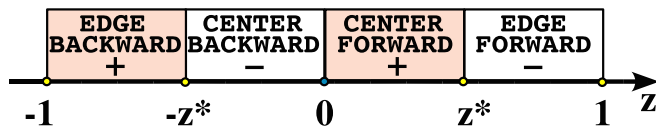

FIG. 3 (color online). The kinematical range of z and the four bins used in the definition of the center-edge-forward-backward asymmetry $A_{CE,FB}$.

due to the fact that the z-dependence of the differential cross section remains the same as in Eq. (2.5) when these interactions add to the SM, the z^*-dependence of $A_{CE,FB}$ will be identical to Eq. (3.12). Namely,

$$A_{CE,FB}^{CI}(z^*) = A_{FB}^{CI}(2z^{*2} - 1). \qquad (3.13)$$

Furthermore, Eqs. (3.12) and (3.13) show that both $A_{CE,FB}^{SM}$ and $A_{CE,FB}^{CI}$ vanish at

$$z^* \equiv z_{CI}^* = 1/\sqrt{2} \approx 0.707, \qquad (3.14)$$

corresponding to $\theta = 45°$.

Stated differently, introducing the deviation of $A_{CE,FB}$ from the SM prediction,

$$\Delta A_{CE,FB} = A_{CE,FB} - A_{CE,FB}^{SM}, \qquad (3.15)$$

in the case of conventional four-fermion contact interactions we have

$$\Delta A_{CE,FB}^{CI}(z^*) = \Delta A_{FB}^{CI}(2z^{*2} - 1), \qquad (3.16)$$

and the expression of A_{FB}^{CI} in terms of helicity amplitudes is formally obtained from Eq. (2.7) by replacing superscripts SM $\rightarrow$ CI. Furthermore,

$$A_{CE,FB}^{SM}(z_{CI}^*) = A_{CE,FB}^{CI}(z_{CI}^*) = \Delta A_{CE,FB}^{CI}(z_{CI}^*) = 0. \quad (3.17)$$

Correspondingly, four-fermion contact interactions are "filtered out" also by the observable (3.10), when measured at $z^* = z_{CI}^*$. One can conclude that $A_{CE,FB} \neq 0$ at z_{CI}^* unambiguously signals the presence of new physics *different* from contact interactions. In Fig. 4, we represent the z^* behavior of $A_{CE,FB}^{CI}$ taking in Eq. (2.12), for illustrative purposes, only the LL among the $\eta_{\alpha\beta}$ as a nonvanishing CI parameter.

Turning to the graviton exchange interaction, the analogue of Eq. (3.4) is

$$A_{CE,FB} = \frac{\sigma_{CE,FB}^{SM} + \sigma_{CE,FB}^{INT} + \sigma_{CE,FB}^{NP}}{\sigma^{SM} + \sigma^{INT} + \sigma^{NP}}, \qquad (3.18)$$

with the same meaning of the superscripts SM, INT, and NP, and in this case, using Eq. (2.10), one can easily see that $\sigma^{INT} = 0$ *and* $\sigma_{CE,FB}^{NP} = 0$.

Thus, for the new physics represented by the KK graviton exchange model, in the approximation of retaining only terms linear in f_G and taking into account Eq. (3.12), one finds for the deviation (3.15) the following expression:

$$\Delta A_{CE,FB}^{ADD}(z^*) = \Delta A_{FB}^{ADD}(2z^{*4} - 1), \qquad (3.19)$$

where

$$\Delta A_{FB}^{ADD}$$
$$= -\frac{3}{4} f_G \frac{\mathcal{M}_{LL}^{SM} + \mathcal{M}_{RR}^{SM} + \mathcal{M}_{LR}^{SM} + \mathcal{M}_{RL}^{SM}}{(\mathcal{M}_{LL}^{SM})^2 + (\mathcal{M}_{RR}^{SM})^2 + (\mathcal{M}_{LR}^{SM})^2 + (\mathcal{M}_{RL}^{SM})^2}.$$
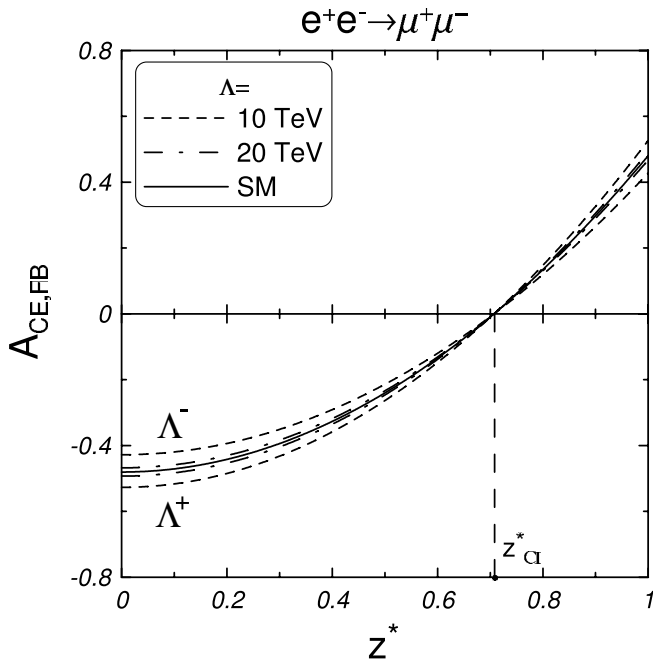$$(3.20)$$

FIG. 4. Center-edge-forward-backward asymmetry $A_{\mathrm{CE,FB}}^{\mathrm{CI}}$ as a function of z^* in the SM (solid line) and in the CI model with $\Lambda^{\pm} = 10$ TeV (dashed lines) and $\Lambda^{\pm} = 20$ TeV (dash-dotted lines). The $\pm$ superscripts correspond to the constructive and destructive interference of the SM amplitudes with the CI ones.
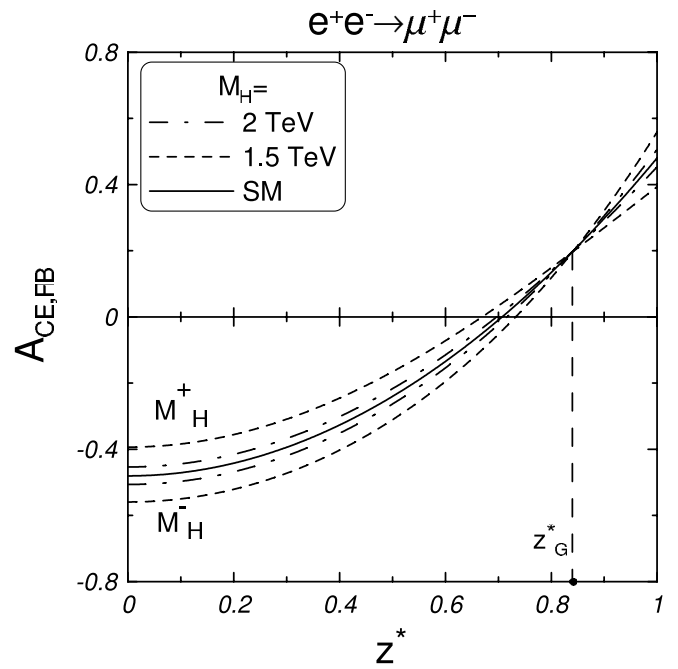

FIG. 5. Center-edge-forward-backward asymmetry $A_{\mathrm{CE,FB}}$ as a function of z^* in the SM (solid line) and in the ADD model with $M_{\bar{H}}^{\pm} = 1.5$ TeV (dashed lines) and $M_{\bar{H}}^{\pm} = 2$ TeV (dash-dotted lines). The $\pm$ superscripts correspond to constructive and destructive interference of the SM amplitudes with the graviton exchange.

Equation (3.19) shows that the deviation of $A_{\mathrm{CE,FB}}$ from the SM prediction vanishes at

$$z_{\mathrm{G}}^* = 1/2^{1/4} \simeq 0.841, \qquad (3.21)$$

corresponding to $\theta = 33°$, i.e., $\Delta A_{\mathrm{CE,FB}}^{\mathrm{ADD}}(z_{\mathrm{G}}^*) = 0$. In Fig. 5 we show the z^* behavior of $A_{\mathrm{CE,FB}}^{\mathrm{ADD}}$ for selected values of the cutoff parameter M_H.

From the remarks above, we conclude that the measurement of $A_{\mathrm{CE,FB}}(z_{\mathrm{G}}^*)$ is sensitive only to new physics induced by four-fermion contact interactions, free of contamination from graviton exchange which does not contribute any deviation from the SM at that value of z^*. Therefore, contributions from CI interactions can unambiguously be identified. Conversely, as being not contaminated by contact interactions, $A_{\mathrm{CE,FB}}(z_{\mathrm{CI}}^*)$ is sensitive only to KK graviton exchange, and can therefore be considered in combination with A_{CE} to enhance the selection power on the ADD scenario.

This suggests, in practice, the kind of analysis exemplified in Fig. 6, where the deviations $\Delta A_{\mathrm{CE,FB}}(z^*)$ for the two scenarios are compared to the statistical uncertainty expected at the Linear Collider. Defining the sensitivity (or the signal statistical significance) to new physics as the ratio between the deviation from the SM and the experimental uncertainty, this figure shows that there is some range of z^* around z_{CI}^* (and extending somewhat below this value) where $\Delta A_{\mathrm{CE,FB}}^{\mathrm{ADD}}$ is appreciably larger than the uncer-
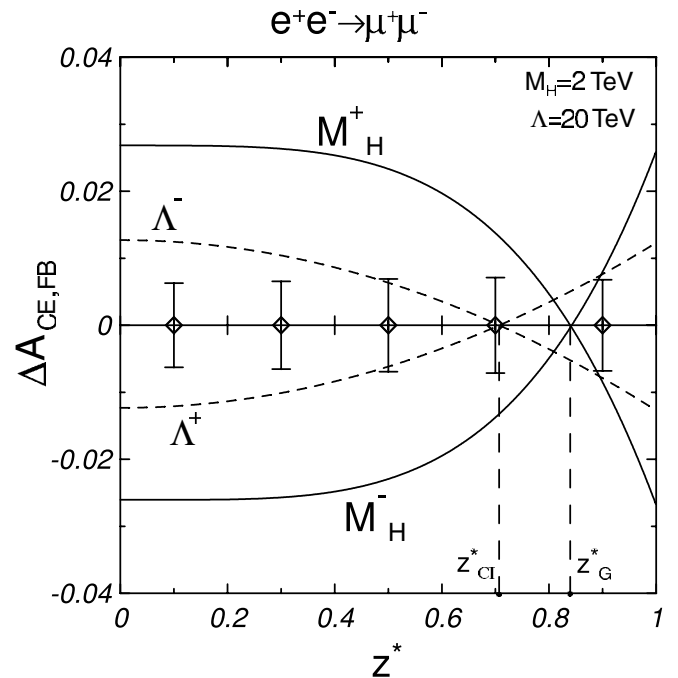

FIG. 6. $\Delta A_{\mathrm{CE,FB}}(z^*)$ in the CI and the ADD scenarios for the indicated values of Λ and M_H. The $\pm$ superscripts refer to positive and negative interference, respectively. The vertical bars represent the statistical uncertainty at an ILC with $\sqrt{s} = 0.5$ TeV and $\mathcal{L}_{\mathrm{int}} = 50$ fb^{-1}.

tainty, while $\Delta A_{\mathrm{CE,FB}}^{\mathrm{CI}}$ is still smaller than (or equal to) the uncertainty. Therefore, in this range, there is maximal sensitivity to the KK graviton exchange. The converse is true in a (limited) range of z^* around z_G^*, where the deviation $\Delta A_{\mathrm{CE,FB}}^{\mathrm{CI}}$ can be dominant, and the sensitivity to contact interactions will be much higher. In general, the widths of the above mentioned z^* intervals will be much larger than the expected experimental uncertainty on z which, therefore, will not affect the numerical results presented in the following sections.

Concerning an analysis based on conventional observables, such as the total cross section σ or the left-right asymmetry A_{LR}, neither of them is sensitive to graviton exchange, because the interference with the SM is there very strongly suppressed (or exactly vanishing if integrated over the full angular range) and the effect would be of higher order in the new physics. The case of the forward-backward asymmetry A_{FB} is reobtained by specializing $A_{\mathrm{CE,FB}}$ to $z^* = 1$ or $z^* = 0$, see Eq. (3.11) and Fig. 6. Therefore, the sensitivities, hence the discovery reaches, can be expected to be comparable. The point is that both graviton exchange and four-fermion contact interactions contribute there, while we are here interested in a clean separation between the two effects. For this reason, we concentrate our analysis around the values of z^* indicated in Fig. 6.

IV. POLARIZED BEAMS

In this case, with P_1 and P_2 the degrees of longitudinal polarization of the electron and positron beams, respectively, we define [28,29]

$$D = 1 - P_1 P_2, \qquad P_{\mathrm{eff}} = \frac{P_1 - P_2}{1 - P_1 P_2}. \qquad (4.1)$$

The polarized differential cross section can be expressed as follows:

$$\frac{d\sigma^{\mathrm{pol}}}{dz} = \frac{D}{4}\left[(1 - P_{\mathrm{eff}})\left(\frac{d\sigma_{\mathrm{LL}}}{dz} + \frac{d\sigma_{\mathrm{LR}}}{dz}\right) + (1 + P_{\mathrm{eff}})\left(\frac{d\sigma_{\mathrm{RR}}}{dz} + \frac{d\sigma_{\mathrm{RL}}}{dz}\right)\right]. \qquad (4.2)$$

The decomposition of the SM polarized differential cross section into z-even and z-odd parts has identical structure as in Eq. (2.5),

$$\frac{d\sigma^{\mathrm{pol,SM}}}{dz} = \frac{3}{8}\sigma^{\mathrm{pol,SM}}(1 + z^2) + \sigma_{\mathrm{FB}}^{\mathrm{pol,SM}}z, \qquad (4.3)$$

and in this case, for the polarized forward-backward asymmetry, Eq. (2.7) is replaced by the following one:

$$A_{\mathrm{FB}}^{\mathrm{pol,SM}} = \frac{3}{4}\frac{(1 - P_{\mathrm{eff}})[(\mathcal{M}_{\mathrm{LL}}^{\mathrm{SM}})^2 - (\mathcal{M}_{\mathrm{LR}}^{\mathrm{SM}})^2] + (1 + P_{\mathrm{eff}})[(\mathcal{M}_{\mathrm{RR}}^{\mathrm{SM}})^2 - (\mathcal{M}_{\mathrm{RL}}^{\mathrm{SM}})^2]}{(1 - P_{\mathrm{eff}})[(\mathcal{M}_{\mathrm{LL}}^{\mathrm{SM}})^2 + (\mathcal{M}_{\mathrm{LR}}^{\mathrm{SM}})^2] + (1 + P_{\mathrm{eff}})[(\mathcal{M}_{\mathrm{RR}}^{\mathrm{SM}})^2 + (\mathcal{M}_{\mathrm{RL}}^{\mathrm{SM}})^2]}. \qquad (4.4)$$

Using Eq. (4.2), one can define the polarized center-edge asymmetry $A_{\mathrm{CE}}^{\mathrm{pol}}$ and the forward–backward–center–edge asymmetry $A_{\mathrm{CE,FB}}^{\mathrm{pol}}$ in exactly the same way as in Eqs. (3.1), (3.2), (3.10), and (3.11), the only difference being that σ must be replaced by σ^{pol} everywhere. Also, the same kind of decomposition into SM, INT and NP contributions as in Eqs. (3.4) and (3.18) can be written for the polarized asymmetries. One can easily see that the z^*-dependence will remain the same as found in the previous sections, while the structure of the z^*-independent factor expressed in terms of the helicity amplitudes will be modified to account for the dependence on the initial electron-positron spin configuration.

A. The polarized center-edge asymmetry $A_{\mathrm{CE}}^{\mathrm{pol}}$

Equations (4.3) and (2.12) immediately show that for the SM as well as for the CI the polarized center-edge asymmetry is the same, and still given by Eq. (3.3) regardless of the c.m. energy and of the values of the beams longitudinal polarization. Therefore, the same considerations made in Sec. III A with regard to the unpolarized case continue to hold, i.e., the center-edge asymmetry will be "transparent" to four-fermion contact interaction effects also for longitudinally polarized beams.

Conversely, for the graviton exchange case, see Eq. (2.10), to first order in the coupling f_G one has instead of Eq. (3.9)

$$\Delta A_{\mathrm{CE}}^{\mathrm{pol,ADD}}(z^*) = \frac{3}{4}f_G\frac{(1 - P_{\mathrm{eff}})(\mathcal{M}_{\mathrm{LL}}^{\mathrm{SM}} - \mathcal{M}_{\mathrm{LR}}^{\mathrm{SM}}) + (1 + P_{\mathrm{eff}})(\mathcal{M}_{\mathrm{RR}}^{\mathrm{SM}} - \mathcal{M}_{\mathrm{RL}}^{\mathrm{SM}})}{(1 - P_{\mathrm{eff}})[(\mathcal{M}_{\mathrm{LL}}^{\mathrm{SM}})^2 + (\mathcal{M}_{\mathrm{LR}}^{\mathrm{SM}})^2] + (1 + P_{\mathrm{eff}})[(\mathcal{M}_{\mathrm{RR}}^{\mathrm{SM}})^2 + (\mathcal{M}_{\mathrm{RL}}^{\mathrm{SM}})^2]}4z^*(1 - z^{*2}). \qquad (4.5)$$

B. The polarized asymmetry $A_{\mathrm{CE,FB}}^{\mathrm{pol}}$

For this observable, the z-integration of the differential cross section (4.2) is the same as in Eqs. (3.10) and (3.11). Of course, also in this case a separation between SM and

NP effects analogous to Eqs. (3.4) and (3.18) holds. Similar to Sec. IV A, the polarized center-edge-forward-backward asymmetries will have the same z^*-dependence as in the unpolarized case, times a z^*-independent factor accounting for the initial beams polarization configuration.

Thus, using the structure of Eqs. (4.2) and (2.12), one finds for the SM and for the contact interactions cases, respectively:

$$A_{\text{CE,FB}}^{\text{pol,SM}}(z^*) = A_{\text{FB}}^{\text{pol,SM}}(2z^{*2} - 1) \quad \text{and}$$
$$A_{\text{CE,FB}}^{\text{pol,CI}}(z^*) = A_{\text{FB}}^{\text{pol,CI}}(2z^{*2} - 1), \tag{4.6}$$

so that the deviation from the SM is given by

$$\Delta A_{\text{CE,FB}}^{\text{pol,CI}}(z^*) = \Delta A_{\text{FB}}^{\text{pol,CI}}(2z^{*2} - 1). \tag{4.7}$$

For graviton exchange, to first order in f_G one finds the relations:

$$A_{\text{CE,FB}}^{\text{pol,ADD}}(z^*) = A_{\text{FB}}^{\text{pol,SM}}(2z^{*2} - 1) + \Delta A_{\text{FB}}^{\text{pol,ADD}}(2z^{*4} - 1), \tag{4.8}$$

or, for the deviation from the SM:

$$\Delta A_{\text{CE,FB}}^{\text{pol,ADD}}(z^*) \cong \Delta A_{\text{FB}}^{\text{pol,ADD}}(2z^{*4} - 1), \tag{4.9}$$

with

$$\Delta A_{\text{FB}}^{\text{pol,ADD}} = -\frac{3}{4} f_G \frac{(1 - P_{\text{eff}})(\mathcal{M}_{\text{LL}}^{\text{SM}} + \mathcal{M}_{\text{LR}}^{\text{SM}}) + (1 + P_{\text{eff}})(\mathcal{M}_{\text{RR}}^{\text{SM}} + \mathcal{M}_{\text{RL}}^{\text{SM}})}{(1 - P_{\text{eff}})[(\mathcal{M}_{\text{LL}}^{\text{SM}})^2 + (\mathcal{M}_{\text{LR}}^{\text{SM}})^2] + (1 + P_{\text{eff}})[(\mathcal{M}_{\text{RR}}^{\text{SM}})^2 + (\mathcal{M}_{\text{RL}}^{\text{SM}})^2]}. \tag{4.10}$$

V. IDENTIFICATION REACHES ON Λ AND M_H

Essentially, to quantitatively discuss the separation of the effects of graviton exchange and contact interactions at the ILC, we can compare the deviations from the SM predictions of the asymmetries defined in the previous sections with the expected experimental uncertainties on these observables.

Summing over $\mu^+\mu^-$, $\tau^+\tau^-$, $b\bar{b}$, and $c\bar{c}$ final states one can perform a conventional χ^2 analysis, with

$$\chi^2 = \sum_{f=\mu,\tau,c,b} \left[\frac{(\Delta A_{\text{CE}}^f)^2}{(\delta A_{\text{CE}}^f)^2} + \frac{(\Delta A_{\text{CE,FB}}^f)^2}{(\delta A_{\text{CE,FB}}^f)^2} \right]. \tag{5.1}$$

Here, ΔA^f represent the deviations from the SM, whose explicit expressions are reported in Secs. III A and III B (and Secs. IV A and IV B in the case of polarized e^+e^- beams), while δA^f are the corresponding expected experimental uncertainties. Basically, numerical constraints on the new physics parameters follow from the condition

$$\chi^2 \leq \chi_{\text{C.L.}}^2, \tag{5.2}$$

where the actual numerical value of $\chi_{\text{C.L.}}^2$ depends on the desired confidence level (C.L.).[5]

The statistical uncertainty is given by

$$\delta A_{\text{i}} = \sqrt{\frac{1 - A_{\text{i}}^2}{\epsilon_f \mathcal{L}_{\text{int}} \sigma}}, \tag{5.3}$$

where $i = \text{CE}$ and CE, FB; $\mathcal{L}_{\text{int}}$ is the integrated luminosity, and ϵ_f denotes the efficiency for reconstruction of the individual $f\bar{f}$ pairs. As numerical inputs, we shall assume the identification efficiencies [31]: $\epsilon_f = 95\%$ for l^+l^- ($l =$

μ, τ); $\epsilon_f = 60\%$ for $b\bar{b}$; $\epsilon_f = 35\%$ for $c\bar{c}$. Specifically, in our numerical analysis we consider an ILC with $\sqrt{s} = 0.5$ TeV and 1 TeV, to assess the dependence of the results on the c.m. energy, and time-integrated luminosity $\mathcal{L}_{\text{int}}$ ranging from 50 up to 1000 fb^{-1}.

Concerning the systematic uncertainties, we assume for the integrated luminosity $\delta\mathcal{L}_{\text{int}}/\mathcal{L}_{\text{int}} = 0.5\%$, and for the electron and positron degrees of longitudinal polarization $|P_1| = 0.8$; $|P_2| = 0.6$, with $\delta P_1/P_1 = \delta P_2/P_2 = 0.5\%$. Since the considered asymmetries are basically determined by ratios of integrated cross sections, one expects systematic errors to cancel to a large extent and, indeed, the uncertainty turns out to be numerically dominated by the statistical one and by the uncertainty on initial beams polarization. On the other hand, as mentioned in Sec. I, the deviations from the SM increase with the c.m. energy $\sqrt{s}$. Therefore, searches on M_H and Λ are favored by the high energies and the high luminosities in e^+e^- collisions envisaged at the planned ILC [26].

In our numerical analysis the angular resolution $\Delta\theta = 0.5$ mrad is assumed, and a 10° angular cut around the beam pipe, i.e., $|z_{\text{cut}}| = 0.98$ is imposed. This kinematical cut leads to the following modifications of the parameters z_0^*, z_{CI}^* and z_{G}^*, see Eqs. (3.8), (3.14), and (3.21):

$$z_0^* = a - a^{-1}, \qquad z_{\text{CI}}^* = \frac{z_{\text{cut}}}{2^{1/2}}, \qquad z_{\text{G}}^* = \frac{z_{\text{cut}}}{2^{1/4}}, \tag{5.4}$$

where $a = [(p + \sqrt{p^2 + 4})/2]^{1/3}$, and $p = (3z_{\text{cut}} + z_{\text{cut}}^3)/2$. The dependence of the reach on M_H and Λ on z_{cut} varying in a reasonable range close to 1 is, for the chosen values of energy, luminosity, and polarization, quite smooth. For example, in the range $z_{\text{cut}} = 0.98 - 1$, the bounds on M_H and Λ are found to vary by some fraction of a percent.

Regarding the theoretical inputs, for the SM amplitudes we use the effective Born approximation [32] taking into account electroweak corrections to the propagators and vertices, with $m_{\text{top}} = 175$ GeV and $m_H = 300$ GeV. Also, $\mathcal{O}(\alpha)$ corrections to process (2.1) are taken into account, along the lines followed in Ref. [7]. Basically,

---

[5]The writing in Eq. (5.1) strictly applies to the case of no correlation between A_{CE} and $A_{\text{CE,FB}}$. Actually, in the numerical analysis such a correlation has been taken into account using the covariance matrix approach [30] and found in practice not influential on the results.

the numerically most important QED corrections, from initial-state radiation, are calculated in the flux function approach (see, e.g., Ref. [33]). To minimize the effect of radiative flux return to the Z whereby the emitted photons peak in the "hard" region $E_\gamma/E_{beam} \approx 1 - M_Z^2/s$, and thus to increase the chances for new physics signals, we apply a cut on the radiated photon energy $\Delta = E_\gamma/E_{beam} < 0.9$. As far as the final-state and initial-final state corrections are concerned, they are evaluated by using ZFITTER [34] and found to be unimportant, for the chosen values of the kinematical cuts, in the derivation of the final numerical results on M_H and Λ. Moreover, the positions of the zeros of the basic asymmetries, z_0^*, z_{CI}^*, and z_G^* [see Eqs. (3.8), (3.14), and (3.21)], can be shifted by the above mentioned QED corrections by a small amount, such that the results of the analysis are practically unaffected.[6]

A. Limits on graviton exchange

In Fig. 7, we show the 5σ identification reach on the graviton exchange mass scale M_H as a function of luminosity and of c.m. energy, obtained from the χ^2 analysis outlined above, combining A_{CE} and $A_{CE,FB}$ at $z^* = z_{CI}^*$. Also, three possible initial beams longitudinal polarization configurations have been considered in this figure. In particular, for A_{CE} ($A_{CE,FB}$) we take $P_1 = P_2 = 0$, $P_1 = 0.8$, $P_2 = 0$ and $P_1 = 0.8$ $P_2 = -0.6$ ($P_1 = P_2 = 0$, $P_1 = -0.8$, $P_2 = 0$ and $P_1 = -0.8$, $P_2 = 0.6$) for the cases of unpolarized beams, polarized electrons, and both beams polarized, respectively, as such values of longitudinal polarizations are numerically found to provide the maximal sensitivity of the asymmetries to M_H. In all three cases the difference between the results for positive and negative interference [$\lambda = \pm 1$ in Eq. (2.10)] are small and cannot be made visible on the scale of the figure.

As one can see, the dependence of the reach on M_H on the luminosity is rather smooth [dimensionally, including the statistical error only, we would expect the bound on M_H to scale like $\sim(\mathcal{L}_{int}s^3)^{1/8}$]. Also, electron and positron longitudinal polarizations can contribute a significant improvement in the sensitivity to graviton exchange, but, at fixed c.m. energy and luminosity, the impact on M_H is not so dramatic due to the high power of the suppression factor $\sim\sqrt{s}/M_H$ in Eq. (2.10), reflecting the dimension-8 relevant operator of Eq. (2.9). This has to be compared with the case of contact interactions, see Eq. (2.12), where the dependence on the suppression factor $\sqrt{s}/\Lambda$ is only quadratic. Also, retaining the statistical uncertainty only, the bound on Λ would scale like $\sim(s\mathcal{L}_{int})^{1/4}$.

It should be interesting to make a comparison of the identification reach derived at the ILC using the kind of analysis described above, with the results on M_H poten-

---

[6]This is true also of the box-diagram contributions, which introduce different angular dependences.
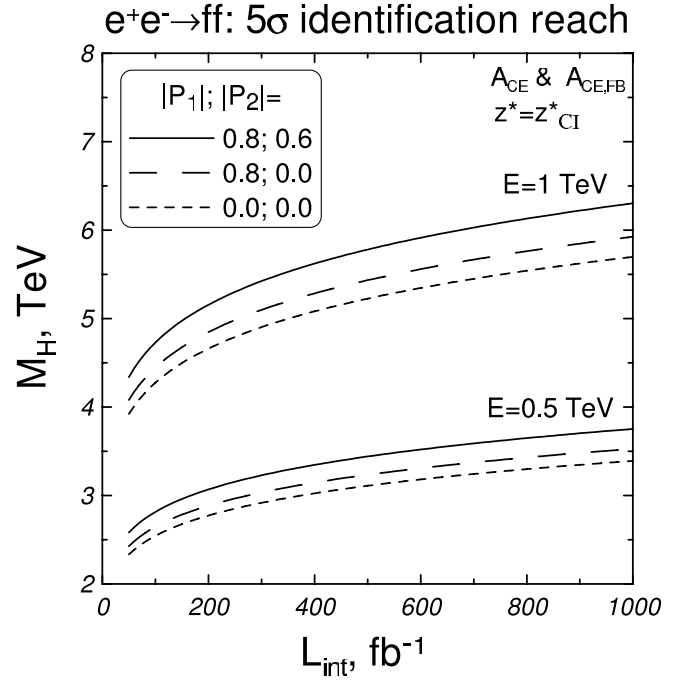

FIG. 7. 5σ identification reach on the mass scale M_H vs integrated luminosity obtained from the combined analysis of two polarized asymmetries, A_{CE} and $A_{CE,FB}$, for the process $e^+e^- \to f\bar{f}$, with f summed over μ, τ, b, c, at $z^* = z_{CI}^*$ and at the c.m. energy of 0.5 TeV and 1 TeV. Short-dashed line: unpolarized; long-dashed line: polarized electrons, $|P_1| = 0.8$; solid line: both beams polarized, $|P_1| = 0.8$, $|P_2| = 0.6$.
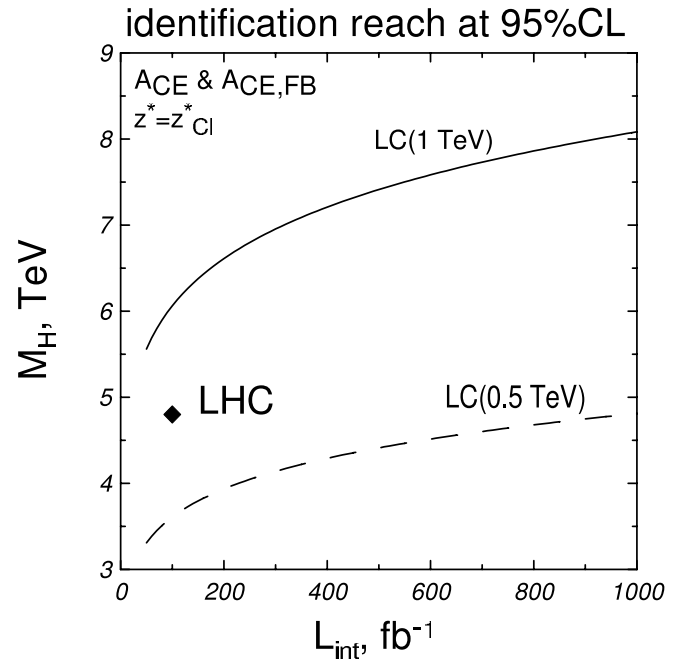

FIG. 8. 95% C.L. identification reach on the mass scale M_H vs integrated luminosity from the dilepton production process at LHC using the center-edge asymmetry and from the processes $e^+e^- \to \bar{f}f$ at ILC for the c.m. energy $\sqrt{s} = 0.5$ TeV and 1 TeV combining A_{CE} and $A_{CE,FB}$ as described in Fig. 7.

tially obtainable from the study of the inclusive dilepton production process

$$p + p \rightarrow l^+ l^- + X, \qquad (5.5)$$

using the observable A_{CE} at the proton-proton collider LHC [8]. This comparison is performed in Fig. 8, which shows the identification reaches at the 95% C.L. obtainable at the ILC for various c.m. energies and luminosities, and at the LHC with $\mathcal{L}_{int} = 100$ fb^{-1}. This figure suggests that the ILC (0.5 TeV) can be competitive to the LHC for $\mathcal{L}_{int} \gtrsim 500$ fb^{-1}, whereas the ILC (1 TeV) is definitely superior for any value of the luminosity.

As repeatedly stressed in Secs. III A and III B, the basic observables A_{CE} and $A_{CE,FB}(z_{CI}^*)$ have the feature that deviations from the SM predictions, if experimentally observed at the ILC within the expected accuracy, can be unambiguously associated to graviton exchange.

In addition, it would be instructive to estimate the precision in the determination of the scale parameter M_H, in the case where the effects of the graviton exchange were observed. Figure 9 shows the uncertainty on M_H for the mass scale varying within the range between the current bound and the expected discovery reach. Of course, this measurement becomes less precise for higher values of the scale parameter.

Since the emphasis is mainly on the basic spin-2 character of the ADD scenario, the above analysis could be applied more generally, also to other extra dimensions graviton (or graviton resonance) exchange models.

Clearly, our "identification" is meant as discrimination of spin-2 graviton effects against those of spin-1 and spin-0 four-fermion contact interactions and, in general, it would not enable us to *a priori* identify extra dimensions models from one another without the addition of more observables.

B. Limits on contact interactions

We now consider the reach on the four-fermion contact-interaction scales Λ defined in Eq. (2.12), obtainable at the linear collider. In Fig. 10, we report the 5σ reach as a function of the time-integrated luminosity and for two options for the c.m. energy, obtained by applying the χ^2 analysis described above to $A_{CE,FB}^{pol}$ at $z^* = z_G^*$, and combining only the final $\mu^+\mu^-$ and $\tau^+\tau^-$ channels. Recall that, as pointed out in Sec. III A, the asymmetry A_{CE} is not sensitive to contact interactions, because the deviation from the SM vanishes. In Fig. 10, the longitudinal polarizations of the initial e^- and e^+ beams leading to maximal sensitivity are specified in the caption. The four curves in each of the two panels are obtained by assuming nonzero values for only one of the $\eta_{\alpha\beta}$ configurations of Eq. (2.11) at a time, and all the others equal to zero (one-parameter fit). As anticipated, the increase of Λ's with $\mathcal{L}_{int}$ is much steeper compared to the case of M_H, reflecting the dimension-6 of the relevant operators.

As discussed in Sec. III B, the values of $\Lambda_{\alpha\beta}$ reported in Fig. 10 should not be contaminated from the effects of
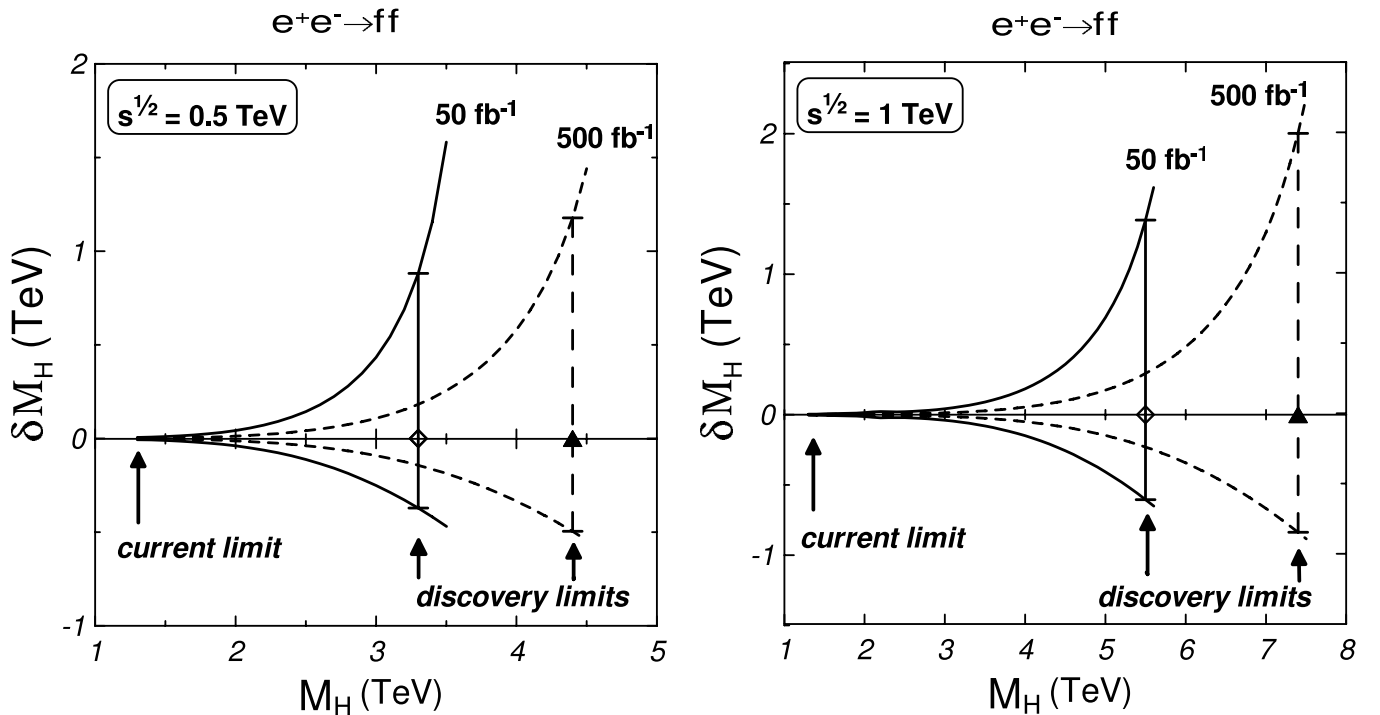

FIG. 9.   Expected uncertainty δM_H (1σ level) on the mass scales vs M_H from the processes $e^+e^- \rightarrow \bar{f}f$ for the c.m. energy $\sqrt{s} = 0.5$ TeV (left panel) and 1 TeV (right panel) combining A_{CE} and $A_{CE,FB}$ as described in Fig. 7.
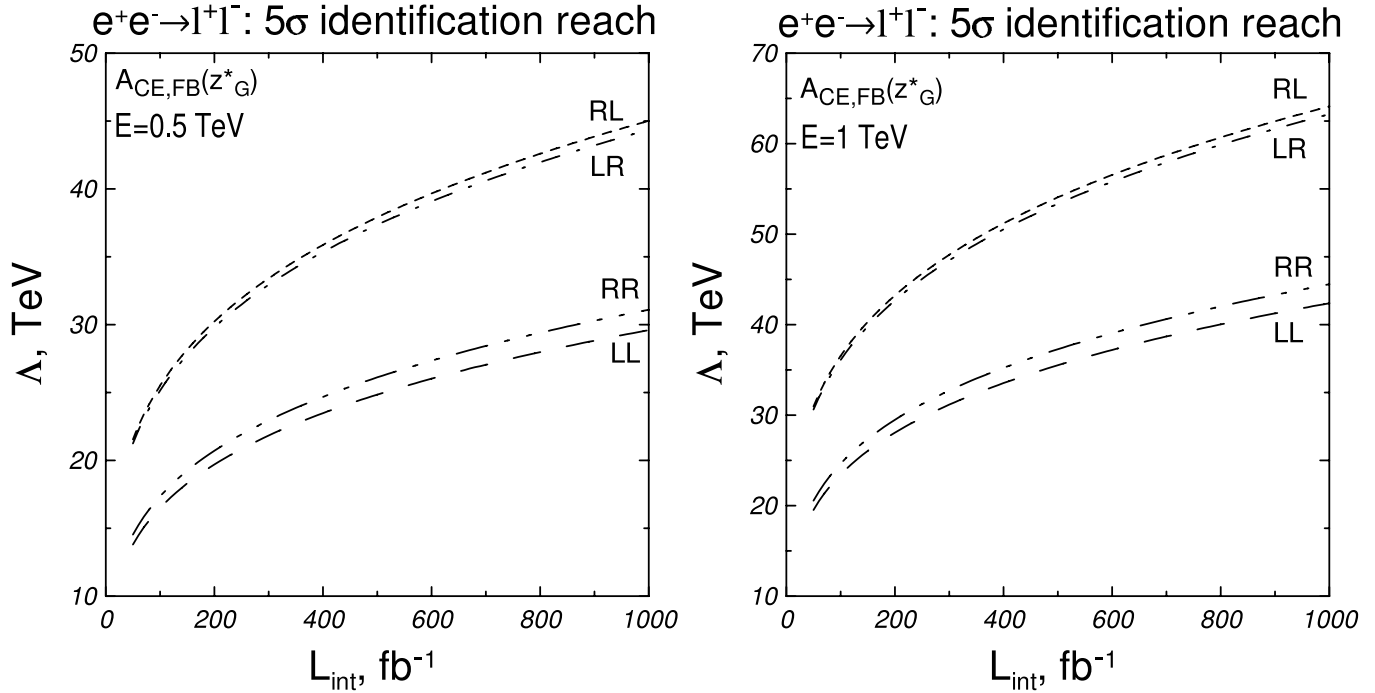
FIG. 10. 5σ reach on the mass scales $\Lambda_{\alpha\beta}$ vs integrated luminosity obtained from the one-parameter fit of polarized center-edge-forward-backward asymmetry $A_{\mathrm{CE,FB}}^{\mathrm{pol}}(z_G^*)$ for the process $e^+e^- \to l^+l^-$, with l summed over μ, τ, at the c.m. energy $\sqrt{s} = 0.5$ TeV (left panel) and 1 TeV (right panel) and $P_1 = 0.8$, $P_2 = -0.6$. Labels attached to the curves indicate the helicity configurations ($\alpha\beta = LL$, RR, LR, RL).
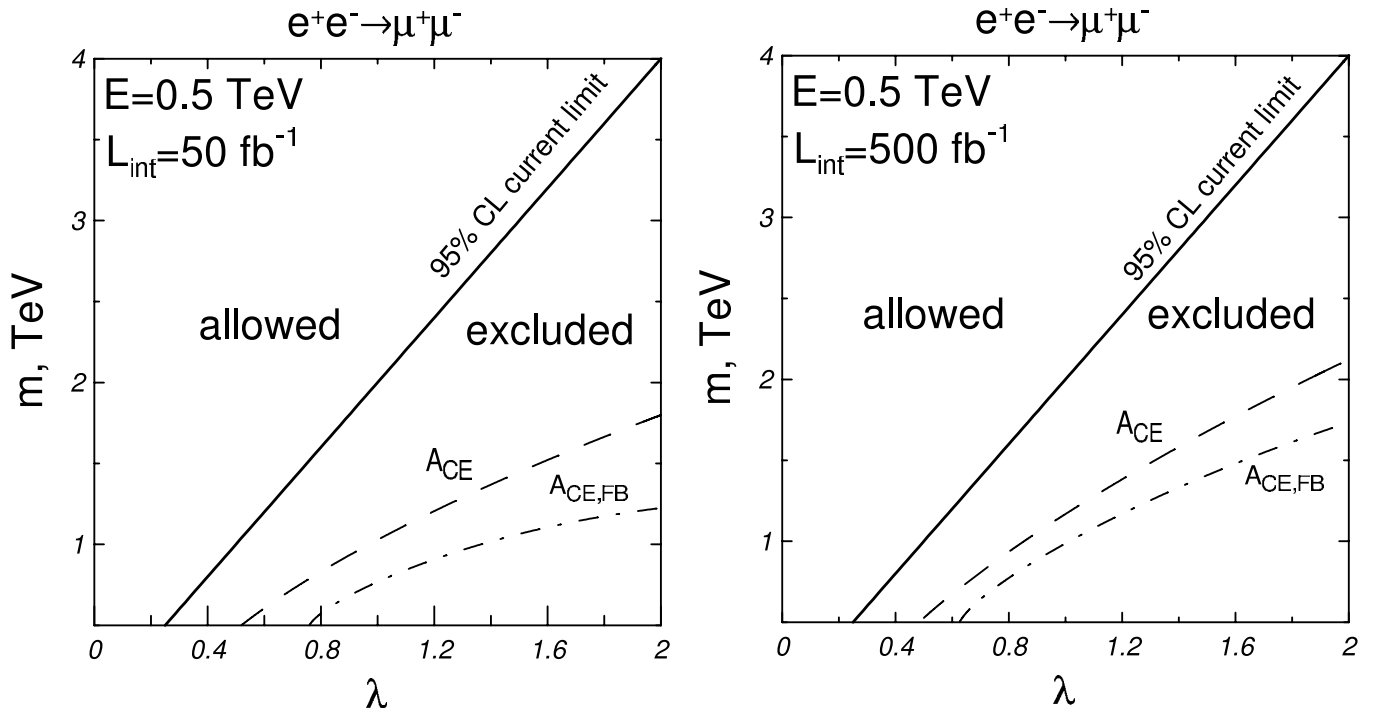

FIG. 11.   Indirect search reach at 95% C.L. for t-channel exchange sneutrino $\tilde{\nu}$ as a function of its mass from the process $e^+e^- \to \mu^+\mu^-$ at $\sqrt{s} = 0.5$ TeV with integrated luminosity $\mathcal{L}_{\mathrm{int}} = 50$ fb^{-1} (left panel) and 500 fb^{-1} (right panel) using $A_{\mathrm{CE,FB}}$ at $z^* = z_{\mathrm{CI}}^*$, $P_1 = -0.8$, $P_2 = 0.6$, and A_{CE} at $z^* = z_0^*$, $P_1 = 0.8$, $P_2 = -0.6$.
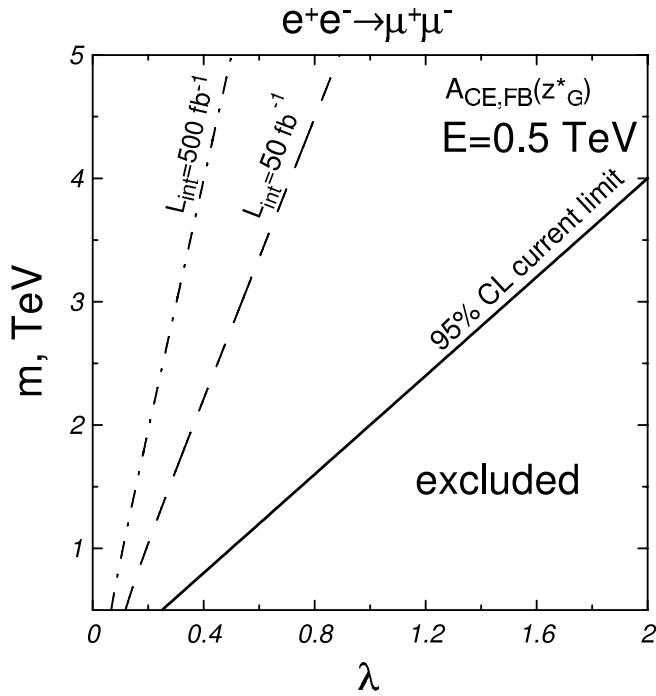
$$e^+e^- \rightarrow \mu^+\mu^-$$

FIG. 12.   Indirect search reach at 95% C.L. for t-channel exchange sneutrino $\tilde{\nu}$ as a function of its mass from the process $e^+e^- \rightarrow \mu^+\mu^-$ at $\sqrt{s} = 0.5$ TeV with integrated luminosity $\mathcal{L}_{\mathrm{int}} = 50$ fb^{-1} (dashed line) and 500 fb^{-1} (dot-dashed line) using $A_{\mathrm{CE,FB}}$ at $z^* = z_{\mathrm{G}}^*$ with $P_1 = -0.8$, $P_2 = 0.6$.

graviton exchange, that vanish in $A_{\mathrm{CE,FB}}$ at $z^* = z_{\mathrm{G}}^*$. On the other hand, as previously remarked, one cannot avoid competitive virtual effects from other kinds of effective 4-fermion interactions, in our case, the chosen example of a very heavy sneutrino exchange in the t-channel, see Eq. (2.13). For an illustration of this effect, in Fig. 11 we report the bounds in the $(\lambda - m)$ plane that we would obtain by considering deviations from the SM of A_{CE} at $z^* = z_0^*$ and of $A_{\mathrm{CE,FB}}$ at $z^* = z_{\mathrm{CI}}^*$ generated from Eq. (2.13). Here, the c.m. energy is $\sqrt{s} = 0.5$ TeV and the integrated luminosity is $\mathcal{L}_{\mathrm{int}} = 50$ and 500 fb^{-1}.[7]

In Fig. 11, the full straight line represents the current limit derived from low-energy physics in Ref. [22]. As one can see, the curves labeled as A_{CE} and $A_{\mathrm{CE,FB}}$ fall far-below the current limit, i.e., the observables $A_{\mathrm{CE}}(z_0^*)$ and $A_{\mathrm{CE,FB}}(z_{\mathrm{CI}}^*)$ are not sensitive to $\tilde{\nu}$-exchange. Indeed, the z-independent contact-interaction limit of Eq. (2.13) cannot contribute to A_{CE} and $A_{\mathrm{CE,FB}}$ at the above mentioned respective values of z^*, and only the remaining, strongly suppressed, t-dependent part would remain to give a non-zero contribution. One therefore can conclude that sneutrino exchange should not contaminate the limits on the graviton scale parameter M_H derived in Sec. VA.

---

[7]We consider only leptonic final states separately because universality is not automatically assured in this framework.

On the other hand, in Fig. 12 we report the bounds in the $(\lambda - m)$ plane that one would obtain by assuming deviations of $A_{\mathrm{CE,FB}}(z_{\mathrm{G}}^*)$ to be generated by Eq. (2.13) instead of (2.12). This figure indicates that at z_{G}^* one cannot unambiguously distinguish the two kinds of new physics, vector-vector contact interactions from sneutrino exchange, so that in the case of four-fermion contact interaction one more appropriately should speak of "discovery reach" rather than "identification reach." On the other hand, the figure shows an interesting possibility to substantially extend the constraints on the sneutrino parameters.

VI. CONCLUDING REMARKS

In the previous sections, we have discussed the possible uses of center-edge asymmetries to pin down spin-2 graviton exchange signatures in the framework of large extra dimensions provided by the ADD model, and our findings can be summarized as follows.

The interference of SM and KK graviton exchanges in process (2.1) produces both $\cos\theta$-even and $\cos\theta$-odd contributions to the angular distribution of outgoing fermions. The appearance of such even and odd new terms does not occur in the case of other new physics, such as the four-fermion contact interactions considered here, and also in some different versions of the extra dimensions framework, for instance the one relevant to gauge boson KK excitations. These interference effects can be directly probed by the center-edge asymmetries, the even ones by A_{CE} and the odd ones by $A_{\mathrm{CE,FB}}$, providing uniquely distinct signatures.

Specifically, the "even" center-edge asymmetry A_{CE} is sensitive *only* to the KK graviton exchange within almost the whole range of the angular kinematical parameter z^* used in its definition. Conversely, the "odd" center-edge-forward-backward asymmetry $A_{\mathrm{CE,FB}}$ is able to project out either conventional four-fermion contact interaction effects or the KK graviton exchange ones by choosing appropriate values of z^*. In particular, $A_{\mathrm{CE,FB}}$ is not affected by spin-2 graviton exchange or by four-fermion contact interactions at $z^* = z_{\mathrm{G}}^* \simeq 0.841$ and at $z^* = z_{\mathrm{CI}}^* \simeq 0.707$, respectively. Accordingly, $A_{\mathrm{CE,FB}}$ can be used to study the identification reach of both the graviton exchange and the conventional contact interactions.

Regarding the numerical limits on the cutoff M_H, using the combination of A_{CE} with the relevant $A_{\mathrm{CE,FB}}$, it is possible to determine spin-2 KK graviton exchange without contamination from the other new physics at the 5σ level up to values of $M_H \sim (6.3 - 7.5)\sqrt{s}$. This represents a substantial improvement over the current situation.

Using this same kind of analysis for the leptonic processes $e^+e^- \rightarrow l^+l^-$, we obtain the 5σ discovery reach for the contact interaction mass scales Λ which range up to 45 TeV and 65 TeV for c.m. energies $\sqrt{s} = 0.5$ TeV and 1 TeV, respectively.

[1] N. Arkani-Hamed, S. Dimopoulos, and G. R. Dvali, Phys. Lett. B **429**, 263 (1998).

[2] N. Arkani-Hamed, S. Dimopoulos, and G. R. Dvali, Phys. Rev. D **59**, 086004 (1999).

[3] I. Antoniadis, N. Arkani-Hamed, S. Dimopoulos, and G. R. Dvali, Phys. Lett. B **436**, 257 (1998).

[4] G. 't Hooft, in *Recent Developments in Gauge Theories*, edited by G. 't Hooft, C. Itzykson, A. Jaffe, H. Lehmann, P. K. Mitter, I. M. Singer, and R. Stora, NATO Advanced Study Institutes, Series B: Physics Vol. 59 (Plenum, New York, 1980); S. Dimopoulos, S. Raby, and L. Susskind, Nucl. Phys. **B173**, 208 (1980).

[5] E. Eichten, K. D. Lane, and M. E. Peskin, Phys. Rev. Lett. **50**, 811 (1983).

[6] R. Rückl, Phys. Lett. B **129**, 363 (1983).

[7] P. Osland, A. A. Pankov, and N. Paver, Phys. Rev. D **68**, 015007 (2003).

[8] E. W. Dvergsnes, P. Osland, A. A. Pankov, and N. Paver, Phys. Rev. D **69**, 115001 (2004).

[9] S. Cullen, M. Perelstein, and M. E. Peskin, Phys. Rev. D **62**, 055012 (2000); G. Pasztor and M. Perelstein, in Proc. of the APS/DPF/DPB Summer Study on the Future of Particle Physics (Snowmass 2001), edited by N. Graf; eConf C010630, P315 (2001); hep-ph/0111471.

[10] T. G. Rizzo, J. High Energy Phys. 10 (2002) 013.

[11] B. Schrempp, F. Schrempp, N. Wermes, and D. Zeppenfeld, Nucl. Phys. **B296**, 1 (1988).

[12] G. F. Giudice, R. Rattazzi, and J. D. Wells, Nucl. Phys. **B544**, 3 (1999).

[13] T. Han, J. D. Lykken, and R. J. Zhang, Phys. Rev. D **59**, 105006 (1999).

[14] J. L. Hewett, Phys. Rev. Lett. **82**, 4765 (1999).

[15] For a review see, e.g., S. Hossenfelder, hep-ph/0409350, and references there.

[16] S. Ask, hep-ex/0410004.

[17] M. K. Ünel (CDF Collaboration and D0 Collaboration), AIP Conf. Proc. No. 753 (AIP, New York, 2005), 400

[18] E. Gallas (D0 Collaboration), FERMILAB-CONF Report No. 04-223.

[19] For a review see, e.g., K. Cheung, hep-ph/0409028.

[20] K. m. Cheung and G. Landsberg, Phys. Rev. D **62**, 076003 (2000).

[21] S. Eidelman *et al.* (Particle Data Group), Phys. Lett. B **592**, 1 (2004).

[22] J. Kalinowski, R. Rückl, H. Spiesberger, and P. M. Zerwas, Phys. Lett. B **406**, 314 (1997); **414**, 297 (1997).

[23] T. G. Rizzo, Phys. Rev. D **59**, 113004 (1999).

[24] A. A. Pankov, N. Paver, and C. Verzegnassi, Int. J. Mod. Phys. A **13**, 1629 (1998).

[25] A. Datta, E. Gabrielli and B. Mele, Phys. Lett. B **552**, 237 (2003).

[26] J. A. Aguilar-Saavedra *et al.* (ECFA/DESY LC Physics Working Group Collaboration), DESY Report No. 01-011; hep-ph/0106315; T. Abe *et al.* (American Linear Collider Working Group Collaboration), in Proc. of the APS/DPF/DPB Summer Study on the Future of Particle Physics, Snowmass, 2001, edited by N. Graf; SLAC Report No. R-570 (2001); hep-ex/0106055.

[27] R. W. Assmann *et al.*, SLAC-CERN Report No. 2000-096; M. Battaglia, A. De Roeck, J. Ellis, and D. Schulte, CERN Report No. 2004-005/2000-008.

[28] K. Flottmann, DESY Report No. 95-064.

[29] K. Fujii and T. Omori, KEK Report No. 95-127.

[30] W. T. Eadie, D. Drijard, F. E. James, M. Roos, and B. Sadoulet, *Statistical Methods in Experimental Physics* (American Elsevier, New York, 1971).

[31] C. J. S. Damerell and D. J. Jackson, in Proceedings of the 1996 DPF/DPB Summer Study on New Directions for High Energy Physics, Snowmass, 1996, edited by D. G. Cassel, L. Trindle Gennari, and R. H. Siemann; Report No. SLAC-R-732 (1996); eConf C960625, DET078 (1996) p. 442.

[32] M. Consoli, W. Hollik and F. Jegerlehner, CERN-TH Report No. 5527-89; G. Altarelli, R. Casalbuoni, D. Dominici, F. Feruglio, and R. Gatto, Nucl. Phys. **B342**, 15 (1990).

[33] For a review see, e.g., W. Beenakker and F. A. Berends, in Proc. of the Workshop Physics at LEP2, (CERN Report No. 96-01), Vol. 1, p. 79 and references therein.

[34] D. Bardin, P. Christova, M. Jack, L. Kalinovskaya, A. Olchevski, S. Riemann, and T. Riemann, Comput. Phys. Commun. **133**, 229 (2001).